

Anti-Bump Switched LPV Control With Delayed Scheduling for Morphing Aircraft

Liang, Ye; Zhang, Lixian; Wang, Xuerui

DOI

[10.1109/TAES.2024.3384177](https://doi.org/10.1109/TAES.2024.3384177)

Publication date

2024

Document Version

Final published version

Published in

IEEE Transactions on Aerospace and Electronic Systems

Citation (APA)

Liang, Y., Zhang, L., & Wang, X. (2024). Anti-Bump Switched LPV Control With Delayed Scheduling for Morphing Aircraft. *IEEE Transactions on Aerospace and Electronic Systems*, 60(4), 5010-5023. <https://doi.org/10.1109/TAES.2024.3384177>

Important note

To cite this publication, please use the final published version (if applicable). Please check the document version above.


Copyright

Other than for strictly personal use, it is not permitted to download, forward or distribute the text or part of it, without the consent of the author(s) and/or copyright holder(s), unless the work is under an open content license such as Creative Commons.

Takedown policy

Please contact us and provide details if you believe this document breaches copyrights. We will remove access to the work immediately and investigate your claim.

Antibump Switched LPV Control With Delayed Scheduling for Morphing Aircraft

YE LIANG , Member, IEEE
Northeast Forestry University, Harbin, China
Harbin Institute of Technology, Harbin, China
Delft University of Technology, Delft, The Netherlands

LIXIAN ZHANG , Fellow, IEEE
Harbin Institute of Technology, Harbin, China

XUERUI WANG 
Delft University of Technology, Delft, The Netherlands

This article is devoted to the antibump switched linear parameter varying (sLPV) controller design for morphing aircraft under delayed scheduling variables (or parameters), which is typically caused by lagging measurements of the morphing extent. Such delayed scheduling is formulated as the control disturbance and the asynchronous control in the sLPV scheme, according to whether the current mode governed by scheduling variables is correctly detected or not. The persistent dwell time (PDT) switching signals are utilized in this article to describe inherent slow and rapid switching phenomena for steady flight and fast morphing, respectively, which is more applicable than the conventional average dwell time (DT) or DT and covers them as special cases. By adopting the detected-mode-based Lyapunov functions and a smooth function, the stability condition is obtained for the underlying system, upon which the antibump sLPV controller allowing for

Manuscript received 12 June 2023; revised 23 November 2023; accepted 26 March 2024. Date of publication 2 April 2024; date of current version 9 August 2024.

DOI. No. 10.1109/TAES.2024.3384177

Refereeing of this contribution was handled by L. Rodrigues.

This work was supported in part by the Natural Science Foundation of China (NSFC) under Grant 62225305 and Grant 12072088, and in part by China Scholarship Council under Grant 202206120240.

Authors' addresses: Ye Liang is with the College of Computer and Control Engineering, Northeast Forestry University, Harbin 150000, China, also with the School of Astronautics, Harbin Institute of Technology, Harbin 150000, China, and also with the Faculty of Aerospace Engineering, Delft University of Technology, 2629HS Delft, The Netherlands, E-mail: (liangye@nefu.edu.cn); Lixian Zhang is with the School of Astronautics, Harbin Institute of Technology, Harbin 150000, China, E-mail: (lixianzhang@hit.edu.cn); Xuerui Wang is with the Faculty of Aerospace Engineering, Delft University of Technology, 2629HS Delft, The Netherlands, E-mail: (x.wang-6@tudelft.nl). (*Corresponding authors: Lixian Zhang; Xuerui Wang.*)

0018-9251 © 2024 IEEE

delayed scheduling is designed, in contrast to the existing studies that simply ignore the detection lag to allow the use of overlapped partitions and scheduling-variable-dependent Lyapunov functions for different modes. By an aircraft with a variable-sweep wing and an aircraft with a deformable wingspan, the effectiveness and the superiority of the proposed approach are demonstrated via simulations.

I. INTRODUCTION

The past decades have witnessed a rapid advance in morphing aircraft [1], [2], [3], which is mainly motivated by its ability of adapting structural configuration to various tasks or environments for superior flight performance and maneuverability. The structure morphing of the aircraft also yields the variation of its dynamic model, such as aerodynamic parameters and center of gravity, indicating that the flight control system of the morphing aircraft is not only nonlinear as the conventional aircraft but also dependent on the current structural configuration. Under such circumstances, the admissible controller with uniform parameters is challenging to be obtained accurately, which motivates the control design for the morphing aircraft to include certain scheduling variables (or parameters in some literature) related to the deformation extent of the structural configuration, especially when the aircraft is with a large-range variation of the structure. However, in practice, the measurements of the deformation extent are likely to be with a time lag due to the detection time demands of sensors, such as piezoelectric sensors [4] or cameras [5], leading to a problem that the corresponding scheduling variables in the designed controllers are delayingly obtained, i.e., delayed scheduling.

Switched linear parameter varying (sLPV) systems, as a powerful tool capable of modeling and control design in a linear manner for nonlinear dynamics, have been extensively utilized in aircraft flight control [6], [7], [8], [9]. In the sLPV scheme for morphing aircraft, the deformation extent of the structure is selected as scheduling variables to obtain the linear control system with parameter-dependent matrices, and the range of scheduling variables is further split into several partitions for the separate control design. Such a method not only improves the solvability but also provides the possibility of control design for various performance at different structural configuration as compared to conventional LPV schemes, especially in the field of aircraft with large-range morphing structure. However, in the scheme of sLPV, the practical problem of delayed scheduling caused by lagging measurements of the deformation extent has not been considered yet. Once the designed controller is scheduled via delayed variables, the system obtains deteriorative performance, and even becomes unstable when the detected partition for controller scheduling is different from the actual partition of the underlying system. The issue of how to design an sLPV scheme allowing for the delayed scheduling and the incorrect partition detection is significant but largely open in the field.

As a kind of switched system, each partition of sLPV is also known as a mode, where the change of the local partition of scheduling variables is converted to the

mode switching. In the existing studies [6], [7], [8], [10], the mode switching of the sLPV system is described by dwell time (DT) or average dwell time (ADT) switching signals. Such slow switching signals require a minimum duration or average minimum duration in one or several modes, respectively, which limits the morphing speed to suppress the maneuverability when the aircraft is required to rapidly change the current structural configuration to the desired one. Persistent dwell time (PDT), as a more general switching signal that covers DT/ADT as special cases [11], has been widely utilized in modeling the system with both slow and rapid switching [9], [12]. However, such a suitable switching signal has not been adopted in flight control of morphing aircraft, despite the evident feature of the underlying system with various switching characteristics that the modes are constant for steady flight and frequently change in the morphing process.

Moreover, since the control gains in the designed sLPV controller are obtained separately for each mode, they will be smoothly scheduled in one mode like common LPV does, but are likely to jump at switching instants of modes. Then, a bump phenomenon arises in control commands, which may be unacceptable and hard to be realized by actuators of the aircraft to correspondingly deteriorate the control performance. To obtain the antibump sLPV controller, in the existing studies [8], [13], an overlapped region is included in the adjacent partitions, then the gains in overlapped regions are obtained by interpolating for a smooth transition. However, as for the case of delayed measurements of scheduling variables, the control gains are hard to be solved via the schemes above since they are designed by requiring the scheduling-variable-dependent or common Lyapunov functions to decrease in all modes, where each mode corresponds to the relatively large-range partition for overlap. Therefore, it is urgent and significant to find a suitable control design method to alleviate the control bump of sLPV accounting for both the aforementioned delayed scheduling and rapid mode switching, which motivates this study.

In this article, the problem of antibump sLPV control design for morphing aircraft with delayed scheduling is investigated. The main contributions are in the following aspects.

- 1) In the sLPV scheme, the phenomenon of delayed scheduling is treated either as the disturbed control inputs or as the asynchronous control of the underlying system, according to whether the detected and the actual mode are matched or not, respectively, which has not been considered before.
- 2) The PDT switching signal is adopted to describe both slow and possible rapid mode switching, which is more applicable for steady flight and fast morphing of the aircraft as compared to existing DT/ADT switching signals.
- 3) The detected-mode-based Lyapunov functions and a smooth function are utilized for stability analysis and antibump sLPV controller design for delayed scheduling, instead of adopting overlapped partition

and scheduling-variable-dependent Lyapunov functions without considering the measurement lag.

The rest of this article is organized as follows. The considered problem is given in Section II, and the sLPV system is modeled in Section III. In Section IV, the control design approaches are obtained, where the advantages and the effectiveness are demonstrated in Section V. Finally, Section VI concludes this article.

NOTATIONS The notations utilized in this article are fairly standard. The superscript T represents matrix transposition, $0^{i \times j}$ stands for the zero matrix with i rows and j columns, $\|\cdot\|$ refers to the Euclidean vector norm, $G \prec H$ indicates that the matrix $G - H$ is negative definite, and \star at (i, j) of the matrix means that it is the transposition of (j, i) in the matrix.

II. PRELIMINARIES AND PROBLEM FORMULATION

Consider the nonlinear dynamic model of a morphing aircraft $\dot{x}(t) = f(x(t), u(t), \xi)$, where $x(t)$ and $u(t)$ are the states and control inputs of the flight control system, while the n -dimensions vector ξ contains the selected scheduling variables, which correspond to the deformation extent of the morphing aircraft. By linearizing the dynamic model at adequate values of ξ , and using the mathematical fitting for each parameter in system matrices, the LPV model of a typical morphing aircraft can be obtained as

$$\dot{x}(t) = A(\xi)x(t) + B(\xi)u(t) \quad (1)$$

where $x(t)$ and $u(t)$ are the increments of the states and control inputs with respect to the trim point of the aircraft at the current scheduling variables ξ , respectively, and $A(\xi)$ and $B(\xi)$ are the Jacobian matrices with appropriate dimensions, which vary as functions of the scheduling variables ξ .

For control design, the underlying system (1) can be further described via the polytopic system approach as $A(\xi) = \sum \varpi A^k$ and $B(\xi) = \sum \varpi B^k$, where $k \in \mathcal{K}$ indicates the k th vertexes corresponding the upper or lower bounds of scheduling variables $\xi \in [\underline{\xi}, \bar{\xi}]$, A^k and B^k are the vertex matrices of the polytopic system, while $\varpi = \prod_{q=1}^{n_\xi} (\xi^q - \underline{\xi}^q) / (\bar{\xi}^q - \underline{\xi}^q)$ are the weights for the convex combination of the polytopic system and ξ^q is one of scheduling variables in the vector ξ . By solving the controller gains K^k of the polytopic system A^k and B^k via state feedback approach, the scheduling variables-dependent stabilizing controller $u(t) = K(\xi)x(t)$ can be obtained by the convex combination of K^k as $K(\xi) = B^{-1}(\xi) \sum \varpi B^k K^k$. However, such an approach requires the same control performance within one polytopic system, which deteriorates the solvability of the controller gains if $\xi \in [\underline{\xi}, \bar{\xi}]$ is of great range, thus motivates the development of sLPV-based approaches [9].

Using the sLPV, the overall range of scheduling variables is split into different partitions to separately design the LPV controller with respect to different control performance, which not only increases the solvability of the

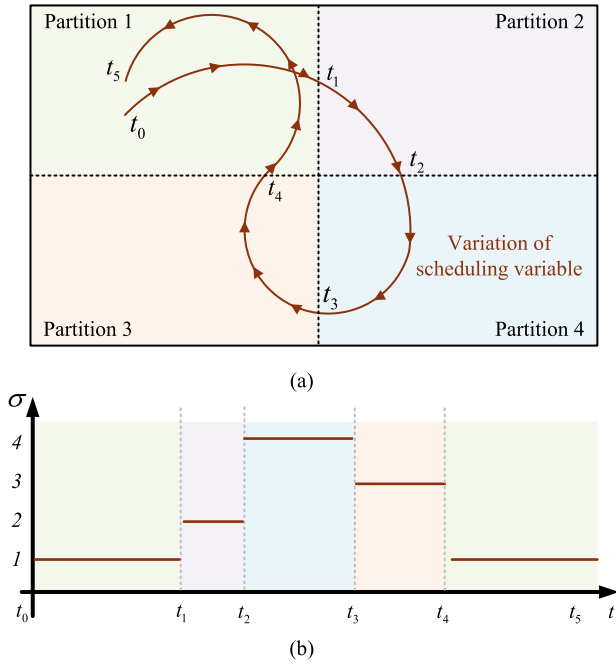


Fig. 1. Illustration of modes and partitions in the scheme of sLPV. (a) Partitions. (b) Modes.

flight controller but also leaves a possibility that the morphing aircraft is with various flight performance at different deformation extent. By modeling the dynamics in each partition as an LPV system and treating it as one mode as the common switched systems scheme does, an sLPV system can be obtained, where the mode evolution is described by a switching signal that jumps when the local partition of scheduling variables changes. A general scenario of sLPV is shown in Fig. 1, where the range of the scheduling variables is split as four partitions, and the corresponding four modes are obtained. Once the scheduling variable crosses the boundary of the partitions, the local partition changes and the mode switches. Thus, the corresponding sLPV can be described as

$$\dot{x}(t) = A_{\sigma(t)}(\xi)x(t) + B_{\sigma(t)}(\xi)u(t) \quad (2)$$

where the switching signal $\sigma(t) \in \mathcal{S} = [1, s]$ is a piecewise and right-continuous function that describes the mode switching, s is the number of modes that equals to the one of the divided partitions of ξ , and the scheduling variables ξ in $A_{\sigma(t)}(\xi)$ and $B_{\sigma(t)}(\xi)$ satisfy $\xi \in [\underline{\xi}_{\sigma(t)}, \bar{\xi}_{\sigma(t)}]$. The system can be stabilized by the sLPV controller $u(t) = K_{\sigma(t)}(\xi)x(t)$ that synchronously switches as modes, where $K_{\sigma(t)}(\xi)$ can be determined by the scheduling variable, the polytopic system of the corresponding partition, and certain switching logic of the switching signal $\sigma(t)$.

In the aforementioned LPV or sLPV approaches, the designed controller is required to be synchronously scheduled according to the current ξ , while the practical and possible delayed scheduling caused by lagging measurements of the deformation extent has not been considered to date, as shown in Fig. 2. Also, for the controller design in the scheme of sLPV in the existing studies, the DT and ADT

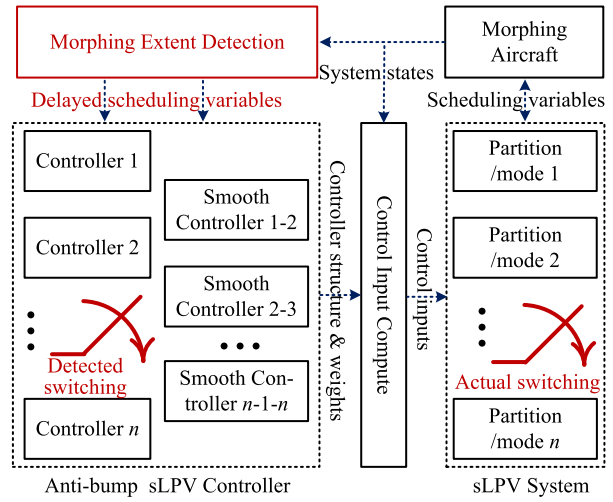


Fig. 2. Illustration of delayed scheduling in the scheme of sLPV via antibump sLPV controller.

switching signals are commonly utilized to describe the mode evolution, which introduces a lower bound to the duration that the scheduling variables cross a partition to limit the morphing speed. In addition, as a common problem in the field of switched systems, the control gains are likely to jump at the switching instants, where the suppression approach shall be reinvestigated in the presence of delayed scheduling and relatively frequent mode switching for possible lagging measurements and rapid morphing of the aircraft, respectively.

The objectives of this article are to formulate a general sLPV model with the consideration of both delayed scheduling and rapid switching, and to design an antibump sLPV controller for morphing aircraft flight control.

III. SLPV SYSTEM FORMULATION

In this section, the sLPV model for the delayed scheduling and antibump control design is first formulated, then the utilized PDT switching signals for description of the rapid morphing of the aircraft are discussed.

A. Antibump sLPV Modeling for Delayed Scheduling

In the sLPV scheme of morphing aircraft, once the scheduling variables denoted by ξ^d are measured with a time lag, the detected mode denoted by $\sigma_d(t)$ is likely to be not the same as the actual mode $\sigma(t)$ since they are determined by the local partition of ξ^d and ξ , respectively, indicating that the adopted controller will be $u(t) = K_{\sigma_d(t)}(\xi^d)x(t)$. Also, considering the requirements of the antibump sLPV controller design, once the mode switching is detected, a duration is required to execute the smooth transition between various controller gains. Then, according to the possible mismatch between the local mode of the scheduled controller based on ξ^d and the actual mode determined by ξ , and considering the smooth transition demands, each mode is split into three modules consisting of *synchronous module*, *asynchronous module*, and *smooth module*, which

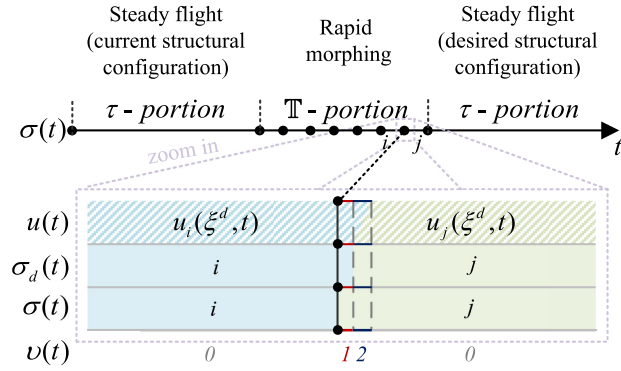


Fig. 3. Illustration of antibump sLPV system with delayed scheduling, where $v(t) = 0, 1$, and 2 refer to the defined synchronous module, asynchronous module, and smooth module, respectively, and the black dots are the actual switching instants of modes.

is denoted by $v(t) = 0, 1$, and 2 , respectively, as shown in Fig. 3.

1) *Synchronous Module*: Although the sLPV controller is delayingly scheduled, it is still in the same mode as the actual one, i.e., $\sigma_d(t) = \sigma(t)$. In the synchronous module of the mode denoted by i , the closed-loop system is given by

$$\begin{aligned}\dot{x}(t) &= A_i(\xi)x(t) + B_i(\xi)K_i(\xi^d)x(t) \\ &= A_i(\xi)x(t) + B_i(\xi)K_i(\xi)x(t) + B_i(\xi)w_{ii}(t) \\ &= A_i(\xi)x(t) + B_i(\xi)u_{ii}(t) + B_i(\xi)w_{ii}(t)\end{aligned}\quad (3)$$

where $u_{ii}(t)$ is the controller via actual scheduling variables that can be easily determined by the convex combination $K_i(\xi) = B_i^{-1}(\xi) \sum \varpi_i B_i^k K_i^k$ from the polytopic system A_i^k, B_i^k of the current mode, and $w_{ii}(t) = (K_i(\xi^d) - K_i(\xi))x(t)$ is the stochastic disturbance acted on the control inputs that are caused by delayed scheduling. Considering that the scheduling variables and the flight states of the morphing aircraft vary with a limited speed in the required range, i.e., $\|\dot{x}(t)\| < \|\bar{x}(t)\|$, $\|x(t)\| < \|\bar{x}(t)\|$, and $\|\dot{\xi}\| < \|\bar{\xi}\|$, it is straightforward that $\|w_{ii}(t)\|$ is bounded in the morphing process.

2) *Asynchronous Module*: The system has already switched into the mode denoted by j , but the used controller is determined by the scheduling variables in the previous mode represented by i , i.e., $\sigma_d(t) \neq \sigma(t)$, which is also named as mode asynchronization in the field of switched systems [14], [15]. Then, the closed-loop system can be obtained as

$$\dot{x}(t) = A_j(\xi)x(t) + B_j(\xi)K_i(\xi^d)x(t) + B_j(\xi)w_{ij}^a(t)\quad (4)$$

where the $w_{ij}^a(t)$ is the disturbance on control inputs at asynchronous module. It is worth noting that the difference between the desired control gains $K_j(\xi)$ and the actual one $K_i(\xi^d)$ is not used here as the synchronous module, which is because that the control gains between different modes may be quite large to obtain great disturbance on control inputs, so that it is more suitable to use the asynchronous control method to analyze the effect as the existing studies do in the

field of switched systems [14]. Also, the disturbance $w_{ij}^a(t)$ is relatively close to but not zero since the control input for flight control is an increment to the trim point, which may introduce slight perturbations on the control inputs (see Example 2 in simulation for more details).

3) *Smooth Module*: This module is included in the system after the asynchronous module to execute the smooth transition of controller gains between adjacent modes when the mode switching is detected, where $\sigma_d(t) = \sigma(t)$ and $\sigma_d(t_0^-) \neq \sigma_d(t_0)$. In this module, a transition controller $u_{ij}^s = f_s(K_i(\xi^b), K_j(\xi^d), x(t))$ will be used, where f_s is the smooth function to be designed and $K_i(\xi^b)$ is the gains at the detected switching instants. The closed-loop system can be obtained by replacing the $u_{ij}(t)$ and $w_{ii}(t)$ in (3) with $u_{ij}^s(t)$ and $w_{ij}^s(t)$, respectively, where $w_{ij}^s(t)$ is related to the smooth function f_s for LPV controllers in adjacent modes and the disturbance $K_j(\xi^d) - K_j(\xi)$ caused by delayed scheduling.

Based on the aforementioned analysis for sLPV via three modules for delayed scheduling and smooth transition, an observer $\dot{x}(t) = Cx(t)$ for states and a filter $\dot{u}(t) = -A_f u(t) + A_f u_c(t)$ for control inputs are introduced to proceed the further control design of the underlying system, then the formulated sLPV system with delayed scheduling for antibump sLPV controller design can be concluded as

$$\begin{aligned}\dot{x}(t) &= A_{\sigma(t)}^c(\xi)x(t) + B^c u_c(t) + B^w w(t) \\ z(t) &= C^c x(t)\end{aligned}\quad (5)$$

where $\sigma(t)$ describes the mode evolution of the system (also the local partition of the current time), $u_c(t)$ is the antibump sLPV controller governed by the detected mode $\sigma_d(t)$ and the defined module $v(t)$ to smoothly transition at the detected switching instants, $A_{\sigma(t)}^c = \begin{bmatrix} A_{\sigma(t)} & B_{\sigma(t)} \\ 0 & -A_f \end{bmatrix}$, $B^c = [0, A_f]^T$, $B^w = B^c$, and $C^c = C$ are the system matrices for further controller design.

REMARK 1 In (5), the scheduling variables related matrices $B_{\sigma(t)}$ are converted to a constant one B^c for further controller design via a filter, which is commonly used in recent studies for complex sLPV system to obtain the controller that strictly ensures the stability of the sLPV system [9], and the dramatic change of actual control input $u(t)$ is relevant to the control bump of the $u_c(t)$ at the switching instant. In addition, for the original sLPV systems with constant $B_{\sigma(t)}$, the filter is not required for the control design.

REMARK 2 The delayed scheduling may also yield slight perturbations on the trim points of states and control inputs in certain flight control systems. The perturbation on control inputs can be also alleviated via the designed controller in this article by considering the H_∞ performance in Section IV, while the one on the states is the uncertainty of the reference, which will cause a small bound related to the difference between the measured reference and the actual one [16] during the morphing process and it will be rapidly eliminated once the morphing process is completed or the morphing extent is accurately measured.

B. Rapid Morphing Description Via PDT Switching Signals

As a hybrid system, the property of mode switching $\sigma(t)$ is quite significant and is widely developed in recent years in the sLPV scheme. Considering the requirements of both rapid morphing and steady flight of the morphing aircraft, the PDT switching signal is utilized in this article, which covers both frequent and slow switching by formulating a switching stage. As shown in Fig. 3, in one switching stage, the mode with a duration larger than a constant τ is formulated in the τ -portion, and the modes with rapid switching of duration less than τ can be formulated in the \mathbb{T} -portion with an upper bound T [14].

Then, for the general scenario of the morphing aircraft, where the aircraft is required to change its structural configuration from the current to the desired one, the morphing process can be formulated within the \mathbb{T} -portion since the scheduling variables rapidly cross certain partitions, and other long-duration flight with constant structural configuration is modeled within the τ -portion since the scheduling variables maintain local partition. By the PDT switching signals, the morphing of structural configuration can be executed as fast as possible, unlike the existing DT/ADT switching signals requiring a lower bound for the duration of modes, resulting in a limited morphing speed.

In the conventional PDT switching signal in the field of switched systems, the \mathbb{T} -portion contains the modes without the lower duration, which, however, a minimum time is practically required for the scheduling variable to pass through a partition and is determined by the physical design of the morphing aircraft. In this article, we assume that the delayed time is relatively slight and less than the actual duration of the modes in the \mathbb{T} -portion, then the rest of the duration in the mode can be used as the smooth module for antibump sLPV controller design. In the p th stage, by denoting the start time of mode 2, 1, and 0 of the $(k+1)$ th mode as $t_{p,k}$, $t_{p,k}^a$, and $t_{p,k}^s$, respectively, and defining the maximum switching times as $N_T + 1$, the PDT switching signal considered in this article is of the conditions including $t_{p+1,0} - t_{p,N_T} = T_p \leq T \leq N_T \tau_p$, $t_{p,1} - t_{p,0} = \tau_p \geq \tau$, $t_{p,k}^s - t_{p,k}^a = T_s$, and $t_{p,k}^a - t_{p,k} \leq \bar{T}_a$, where \bar{T}_a and T_s are the upper bounds of the time lag of delayed scheduling and designed duration for control transition, respectively.

REMARK 3 This article considers the general case that the morphing aircraft rapidly and smoothly changes its current structural configuration to the desired one, where the phenomenon that the scheduling variable frequently moves back and forth at the boundary of the partition is avoided.

REMARK 4 Since there exists an upper-bounded duration for the morphing process, the disturbance $w(t)$ will still be bounded even if $x(t)$ increases in the extreme case that the system is unstable caused by largely delayed scheduling.

IV. CONTROL SYNTHESIS

In this section, the stability conditions and the H_∞ performance of the underlying system are first derived, upon

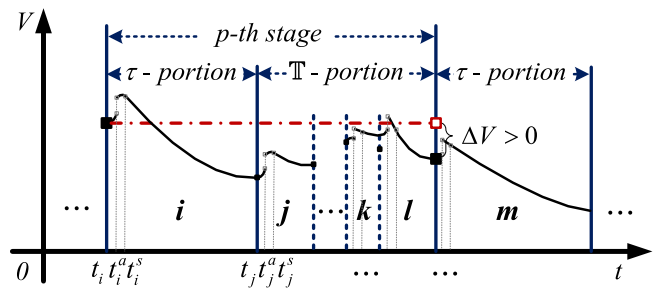


Fig. 4. Illustration of energy variation of the formulated antibump sLPV scheme for delayed scheduling via detected-mode-based Lyapunov functions.

which the antibump sLPV controller is designed for the morphing aircraft control with delayed scheduling.

A. Stability Analysis

Let us first derive the stability conditions of the formulated nominal antibump sLPV system (5) for morphing aircraft with delayed scheduling. By splitting equally the smooth module as n_s intervals for further control design, the following stability condition can be obtained.

LEMMA 1 For the sLPV system (5) without disturbance, let $\mu_{ij} > 1$, $\varrho_i > 0$, $\varepsilon_{ij} \geq -\varrho_i$, and $\vartheta_{ij}^m \geq -\varrho_j$ be given constants. If there exist positive-definite functions $V_{\sigma_d(t)}$, and two class \mathcal{K}_∞ functions κ_1 and κ_2 , such that for any mode switching occurs from mode i to j

$$\begin{aligned} \kappa_1(\|x(t)\|) &\leq V_{\sigma_d(t)}(x(t)) \leq \kappa_2(\|x(t)\|) \quad \forall t \geq 0 \\ \dot{V}_i(x(t)) &\leq -\varrho_i V_i(x(t)), \quad v(t) = 0 \\ \dot{V}_i(x(t)) &\leq \varepsilon_{ij} V_i(x(t)), \quad v(t) = 1 \\ \dot{V}_j(x(t)) &\leq \vartheta_{ij}^m V_j(x(t)), \quad v(t) = 2, s(t) = m \\ V_j(x(t)) &\leq \mu_{ij} V_i(x(t)), \quad \sigma_d(t) = j, \sigma_d(t^-) = i \end{aligned} \quad (6)$$

where $s(t)$ is a piecewise and right continuous function and its value $m \in [0, n_s - 1]$ refers to the $(m+1)$ th intervals in the smooth module. Then, the sLPV system (2) without disturbance is said to be globally uniformly asymptotically stable (GUAS) under any PDT switching signals satisfying

$$\tau > \frac{f}{\underline{\varrho}} [\ln \bar{\mu} + \bar{T}_a(\bar{\varepsilon} + \underline{\varrho}) + T_s \Xi(\underline{\varrho}, \bar{\vartheta}^m, n_s)] - T_{as} \quad (7)$$

where $\Xi(\underline{\varrho}, \bar{\vartheta}^m, n_s) = \sum_{k=0}^{n_s-1} (\underline{\varrho} + \bar{\vartheta}^m)$, $f = N_T + 1$, $T_{as} = N_T(T_s + \bar{T}_a)$, $\underline{\varrho}$, $\bar{\mu}$, $\bar{\varepsilon}$, and $\bar{\vartheta}^m$ are the minimum and maximum of variables ϱ_i , μ_{ij} , ε_{ij} , and ϑ_{ij}^m , respectively.

PROOF The main method is to ensure the system energy described by detected-mode-based Lyapunov functions decreases in each stage, and the details can be found in the Appendix.

A scenario of the energy variation of the underlying system is shown in Fig. 4, where the detected-mode-based Lyapunov functions $V_{\sigma_d(t)}$ are utilized for the system energy description for the solvability of the controller gains [15] in the case of delayed scheduling. Also, in the smooth module,

since the gains are smoothly transitioned, the duration T_s is split equally into n_s intervals such that the converge rate is sampled at different instants, which is beneficial for further design of antibump controller in the continuous-time switched systems scheme (see Theorem 1 for more details). In addition, compared to the common asynchronous PDT switching [14], in Lemma 1, the converge rate ε_{ij} of the asynchronous module can be set near to $-\varrho_i$ instead of being strictly positive since the system matrices are also dependent on the scheduling variables that with a relatively slight change at the asynchronous module near the switching instants.

Now, we turn to the H_∞ performance analysis of the formulated antibump sLPV system for delayed scheduling for morphing aircraft flight control, where the H_∞ performance expressed by the \mathcal{L}_2 gain γ is defined by $\int_{t_0}^{\infty} \|z(t)\|^2 dt \leq \gamma \int_{t_0}^{\infty} \|w(t)\|^2 dt$ under zero initial conditions [17], then the following Lemma can be obtained.

LEMMA 2 For the sLPV system (5), let $\mu_{ij} > 1$, $\varrho_i > 0$, $\varepsilon_{ij} \geq -\varrho_i$, and $\vartheta_{ij}^m \geq -\varrho_j$ be given constants. If there exist positive-definite functions $V_{\sigma_d(t)}$, two class \mathcal{K}_∞ functions κ_1 and κ_2 , and a scalar $\gamma_0 > 0$ such that for any mode switching from i to j

$$\begin{aligned} \kappa_1(\|x(t)\|) &\leq V_{\sigma_d(t)}(x(t)) \leq \kappa_2(\|x(t)\|) \quad \forall t \geq 0 \\ \dot{V}_i(x(t)) &\leq -\varrho_i V_i(x(t)) - \Gamma(t), \quad v(t) = 0 \\ \dot{V}_i(x(t)) &\leq \varepsilon_{ij} V_i(x(t)) - \Gamma(t), \quad v(t) = 1 \\ \dot{V}_j(x(t)) &\leq \vartheta_{ij}^m V_j(x(t)) - \Gamma(t), \quad v(t) = 2, s(t) = m \\ V_j(x(t)) &\leq \mu_{ij} V_i(x(t)), \quad \sigma_d(t) = j, \sigma_d(t^-) = i \end{aligned} \quad (8)$$

where $\Gamma(t) = z^T(t)z(t) - \gamma_0 w^T(t)w(t)$. Then, the sLPV system (2) is GUAS and has a nonweighted \mathcal{L}_2 -gain (non-weighted H_∞ performance) no greater than $\gamma = c\gamma_0$ under the PDT switching signals satisfying (7), and

$$c = \sqrt{\frac{\underline{\varrho} \bar{\mu}^f e^{\underline{\varrho}(\underline{\varrho} + \bar{\varepsilon})f\bar{T}_a + f\Xi(\underline{\varrho}, \bar{\vartheta}^m, n_s)T_s}}{\underline{\varrho} - \frac{f}{\mathbb{T}} \ln \bar{\mu} - (\underline{\varrho} + \bar{\varepsilon}) \frac{f}{\mathbb{T}} \bar{T}_a - \frac{f}{\mathbb{T}} \Xi(\underline{\varrho}, \bar{\vartheta}^m, n_s)T_s}} \quad (9)$$

where $\mathbb{T} \geq \tau + T_{as}$ is the actual minimum duration of one switching stage.

PROOF The main method is to analyze the time integration of the disturbance $w(t)$ and the observer output $z(t)$, and the details can be found in the Appendix.

From Lemma 2, it is straightforward that the H_∞ performance will be deteriorated by largely delayed scheduling and long-time control transition, i.e., increasing \bar{T}_a or T_s , while it can be improved by increasing the PDT τ .

REMARK 5 The parameter c for H_∞ performance expression is always a real number since both numerator and denominator of the fraction under the root number are positive real numbers. The value of the numerator can be readily checked to be greater than 0 since $\underline{\varrho} > 0$, while the value of the denominator to be positive can be ensured by the PDT condition (7).

B. Controller Design

This subsection is devoted to the antibump controller design for morphing aircraft allowing for delayed scheduling based on the obtained stability condition and H_∞ performance. To facilitate the expression, the notations $A_{\sigma(t)}^c(\xi)$, B^c , u^c , and C^c in (5) are denoted as $A_{\sigma(t)}(\xi)$, B , u , and C , respectively, in the following development. For $\forall i, j \in \mathcal{S}$, let A_i^k be the vertexes of the partition \mathcal{A}_i of mode i , A_{ij}^{sk} are the vertexes of the maximum partitions \mathcal{A}_{ij}^s related to the maximum delayed time \bar{T}_a and morphing speed when scheduling from i to j , and A_{ij}^{sk} are the vertexes of the polytopic system of the smooth module \mathcal{A}_{ij}^s determined by given smooth time T_s , $\chi(t)$ is a smooth function that monotonously increases in the smooth module with initial value of 0 and final value of 1. Apparently, the polytopic system for the switching from i to j satisfies $\mathcal{A}_{ij}^a \subset \mathcal{A}_{ij}^s \subseteq \mathcal{A}_j$, since \mathcal{A}_{ij}^s should cover any $T_a \leq \bar{T}_a$. Then, the antibump sLPV controller for delayed scheduling can be obtained by the following theorem.

THEOREM 1 For the sLPV system (5), let $\mu_{ij} > 1$, $\varrho_i > 0$, $\varepsilon_{ij} \geq -\varrho_i$, and $\vartheta_{ij}^m \geq -\varrho_j$ be given constants. If there exist positive-definite symmetric matrices X_i , matrices W_i^k , and $\gamma_0 > 0$, such that for $\forall \sigma(t) = i, j \in \mathcal{S}$, ($i \neq j$) and $\forall k, r \in \mathcal{K}$

$$\begin{aligned} \mathcal{H}(A_i^k X_i + B W_i^k + X_i A_i^{kT} + W_i^{kT} B^k + \varrho_i X_i, X_i) &< 0 \\ \mathcal{H}(A_{ij}^{sk} X_i + B W_i^r + X_i A_{ij}^{skT} + W_i^{rT} B^T - \varepsilon_{ij} X_i, X_i) &< 0 \\ X_i &< \mu_{ij} X_j \end{aligned} \quad (10)$$

and exists a function $\chi(t)$ satisfying $\chi(0) = 0$, $\chi(m \frac{T_s}{n_s}) \leq \chi((m+1) \frac{T_s}{n_s})$, $\chi(T_s) = 1$ such that $\vartheta_{ij}^m = \chi(m \frac{T_s}{n_s}) \varrho_i - (1 - \chi(m \frac{T_s}{n_s})) \mu_{ij}^s$, and μ_{ij}^s satisfies

$$\mathcal{H}(A_{ij}^{sk} X_j + B W_{ij}^r + X_j A_{ij}^{skT} + W_{ij}^{rT} B - \mu_{ij}^s X_j, X_j) < 0 \quad (11)$$

where $W_{ij}^r = \sum \varpi_i(\xi_{ij}^b) K_i^r X_j$, $\varpi_i(\xi_{ij}^b)$ is the weights of the partition i on the boundary between i and j , and

$$\mathcal{H}(\Phi, X_i) = \begin{bmatrix} \Phi & B^w & X_i C^T \\ \star & -\gamma_0^2 I & 0 \\ \star & \star & -I \end{bmatrix}. \quad (12)$$

Then, the system will be GUAS with nonweighted H_∞ performance (9) under any PDT switching signals satisfying (7). In addition, if there exist admissible solutions for the inequalities (10) and the function $\chi(t)$, the antibump sLPV controller with delayed scheduling can be designed as

$$u_{\sigma_d(t)} = \begin{cases} \sum \varpi_i(\xi^d) K_i^k, & v(t) = 0, 1 \\ \chi(t) \sum \varpi_j(\xi^d) K_j^k + (1 - \chi(t)) \sum \varpi_i(\xi_{ij}^b) K_i^k, & v(t) = 2 \end{cases} \quad (13)$$

where $K_i^k = W_i^k X_i^{-1}$.

PROOF The main idea is to carry out the necessary conditions in Lemmas 1 and 2 via Schur complements of (10) and (11), where the details can be found in the Appendix.

Based on the detected-mode-based Lyapunov functions, it is straightforward that we can readily design the control

gains for scheduling in different modes via (11), and then find μ_{ij}^s satisfying (13). In such a scenario, any function $\chi(s(t))$ that monotonously increases from 0 to 1 within smooth time T_s can be used, then the PDT condition and the nonweighted H_∞ performance for flight stability can be computed by $T_s \Xi(\underline{q}, \vartheta^m, n_s)$ with sampling times n_s , where the required τ tend to decrease as n_s increases.

As for the case of control design for a given duration condition of different modes in morphing process, Theorem 1 can also be used by a pre-given factor μ_{ij}^s by virtue of the split intervals in smooth module for computation of $T_s \Xi(\underline{q}, \vartheta^m, n_s)$. Specifically, under such circumstances, a pre-given μ_{ij}^s is used and $\vartheta_{ij}^m = \mu_{ij}^s$ is considered for parameter setting for PDT conditions in controller design. If the controller designed by (10) satisfies (11), the antibump controller can be obtained by any monotonously increasing $\chi(t)$ between $[0, 1]$. Otherwise, a $\vartheta^0 = \overline{\mu_{ij}^s} > \mu_{ij}^s$ is obtained, then the smooth function can be determined by increasing the sample times n_s and flexibly adapting ϑ^m until the total energy variation speed in the smooth module $T_s \Xi(\underline{q}, \vartheta^m, n_s)$ be less than the predesigned $T_s \Xi(\underline{q}, \mu_{ij}^s, 1)$.

REMARK 6 By virtue of the asynchronous module considered in this article, the act on the j of controller gains $K_j(\xi_{ij}^b)$ is considered. Then, μ_{ij}^s can be easily designed via the given constant for the asynchronous module, so that the computed μ_{ij}^s is typically smaller than pre-given μ_{ij}^s .

REMARK 7 Consider the form of the designed antibump sLPV controller for delayed scheduling (13), the disturbance on control inputs (5) in the smooth module can be expressed as $w_{ij}^s(t) = \chi(t)(K_j(\xi^d) - K_j(\xi))x(t)$.

REMARK 8 In this article, the utilization of the detected-mode-based Lyapunov functions in the scheme of the polytopic system of sLPV not only reduces the difficulty of controller solving but also covers the issue of delayed scheduling, unlike the existing scheduling-variables-dependent Lyapunov functions [8], [13], where a large number of inequalities shall be solved and the issue of delayed scheduling is ignored.

REMARK 9 The proposed approach treats the conventional sLPV controller design methods as special cases. The sLPV controller considering H_∞ performance can be designed by solving the first and the third inequalities of (10) in Theorem 1 (see [9] for more details). By ignoring the H_∞ performance, $\mathcal{H}(A_i^k X_i + B W_i^k + X_i A_i^{kT} + W_i^{kT} B^k + Q_i X_i, X_i) < 0$ in Theorem 1 can be modified as $A_i^k X_i + B W_i^k + X_i A_i^{kT} + W_i^{kT} B^k + Q_i X_i < 0$, then the corresponding sLPV controller can be obtained by solving the inequality together with $X_i < \mu_{ij} X_j$.

REMARK 10 In this article, the asynchronous module between adjacent modes is considered, as shown in Fig. 3 and Theorem 1. Then, the delay of scheduling variables can be handled when the delayed scheduling variable and the actual scheduling variable are in the adjacent partitions. Also, the robustness of the proposed controller is quantitatively evaluated by the nonweighted \mathcal{L}_2 -gain, which describes the

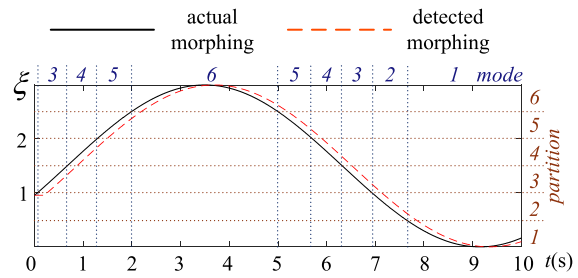


Fig. 5. Illustration of actual and detected morphing of *Firebee*, which is described by actual and detected variation of scheduling variable, respectively.

robustness to not only the delayed scheduling but also the uncertainties on control inputs.

V. SIMULATION

In this section, two classes of typical morphing aircraft described by the LPV model and the original dynamic model, respectively, are considered to demonstrate the effectiveness and the advantages of the proposed antibump sLPV controller for morphing aircraft in the presence of delayed scheduling.

A. Example 1: LPV Model of *Firebee*

The LPV model of morphing aircraft named *Firebee* [18] with a variable-sweep wing is adopted, where the scheduling variable $\xi = (\nu - 15)/\nu \in [0, 3]$ is defined by the angle of the sweep wing ν with respect to its range $\nu \in [15 \text{ deg}, 60 \text{ deg}]$, then the short-period LPV model can be described as [8]

$$\begin{bmatrix} \Delta \dot{\alpha} \\ \Delta \dot{q} \end{bmatrix} = \begin{bmatrix} a_{11}(\xi) & 1 \\ a_{21}(\xi) & a_{22}(\xi) \end{bmatrix} \begin{bmatrix} \Delta \alpha \\ \Delta q \end{bmatrix} + \begin{bmatrix} b_{11}(\xi) \\ b_{21}(\xi) \end{bmatrix} \Delta \delta_e \quad (14)$$

where the expression of $a_{11}(\xi)$, $a_{21}(\xi)$, $a_{22}(\xi)$, $b_{11}(\xi)$, and $b_{21}(\xi)$ can be found in the Appendix; α , q , and δ_e are the attack angle, angle velocity, and elevator deflection, respectively. By the filter of control input $\Delta \dot{\delta}_e = -k_f \Delta \delta_e + k_f \Delta \delta_{ec}$ with $k_f = 1$, the LPV model (14) is converted to

$$\begin{bmatrix} \Delta \dot{\alpha} \\ \Delta \dot{q} \\ \Delta \delta_e \end{bmatrix} = \begin{bmatrix} A(\xi) & B(\xi) \\ 0^{1 \times 2} & -k_f \end{bmatrix} \begin{bmatrix} \Delta \alpha \\ \Delta q \\ \Delta \delta_e \end{bmatrix} + \begin{bmatrix} 0^{2 \times 1} \\ k_f \end{bmatrix} \Delta \delta_{ec} \quad (15)$$

where $A(\xi)$ and $B(\xi)$ can be derived from (14), and δ_{ec} is the virtual control input to be designed, which is also known as the next-level actuator of the elevator [19].

Here, we consider a test scenario that the aircraft continuously changes its structural configuration under nonzero initial conditions to verify the effectiveness and advantages of the developed controller on transient performance. The angle variation of the sweep wing is governed by $\xi = 1.5 \sin(t/1.8 + 1.2 - \pi/2) + 1.5$, and the maximum delayed time of measurements is 0.2 s, as shown in Fig. 5. The LPV system (15) is formulated as the sLPV system with six modes, where the range of the scheduling variable ξ is split equally to obtain the corresponding six partitions, i.e., $\xi_i \in [0.5i - 0.5, 0.5i]$ in the mode $i \in [1, 6]$. Then the

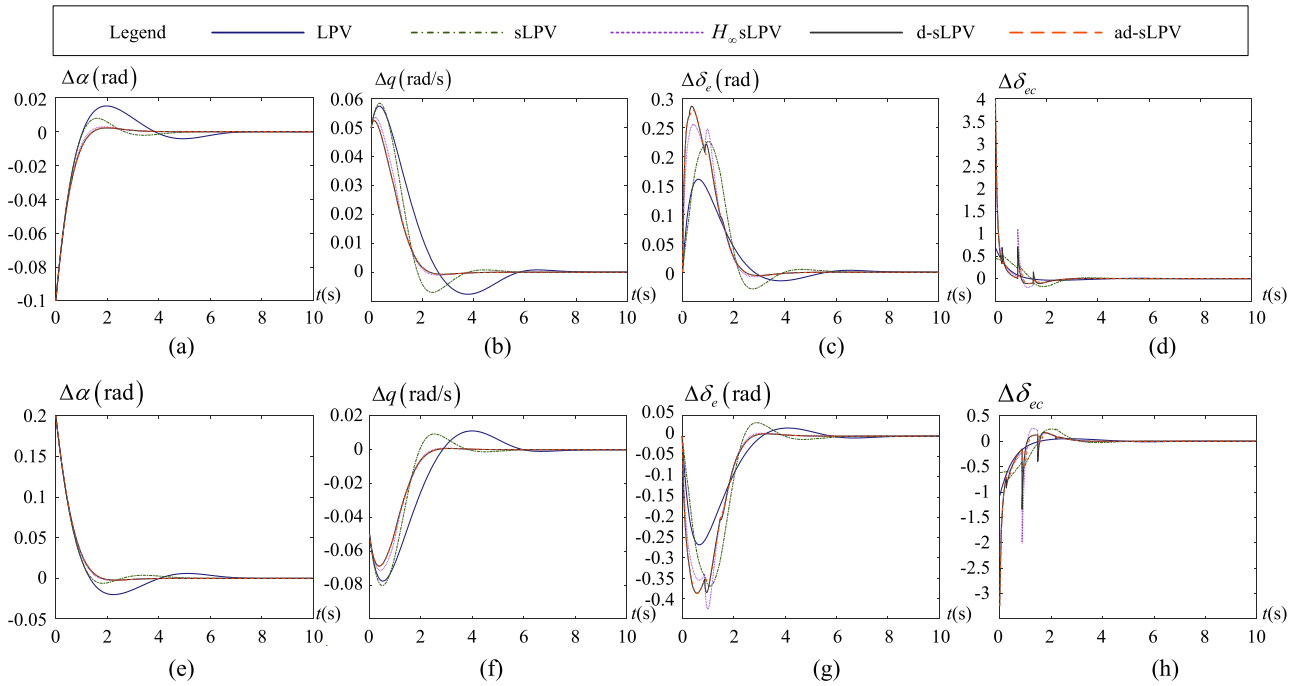


Fig. 6. State response and control inputs of the Firebee with delayed scheduling under various initial values, where the utilized controllers are designed by the schemes include the common LPV, sLPV, and H_∞ sLPV in previous studies, and d-sLPV (sLPV considering delayed scheduling) and ad-LPV (antibump sLPV considering delayed scheduling) in this article. The subfigures (a)–(d) and subfigures (e)–(h) are obtained with the initial conditions $[-0.1, 0.05]^T$ and $[0.2, -0.05]^T$, respectively. (a) Attack angle. (b) Velocity of attack angle. (c) Elevator deflection. (d) Actuator input. (e) Attack angle. (f) Velocity of attack angle. (g) Elevator deflection. (h) Actuator input.

modes 1 and 6 are with long duration while others are with relatively short duration.

The antibump sLPV controller for delayed scheduling denoted by ad-sLPV is designed via Theorem 1 using $\mu_{ij} = 1.5$, $[\varrho_1, \varrho_2, \varrho_3, \varrho_4, \varrho_5, \varrho_6] = [2, 0.8, 0.8, 0.5, 0.5, 2]$, $\gamma_0^2 = 0.1$ that has been optimized, $\varepsilon_{ij} = -\varrho_i + 0.1$, smooth function $\chi(t) = \sin[\frac{(t-t_0)}{T_s} \cdot \frac{\pi}{2}]$ with $T_s = 0.2$ s, where the asynchronous module covers 60% of the total partition to be reached, to obtain the PDT condition $\tau > 2.8547$ and H_∞ performance $\gamma < 2.7647$ for the actual morphing process. Three controllers in existing studies are utilized for comparison, including common LPV [20], sLPV [7], H_∞ sLPV developed in literature [9]. The common LPV controller is designed via $\varrho = 0.5$, while the utilized parameters ϱ_i , μ_{ij} in sLPV and ϱ_i , μ_{ij} , γ_0 in H_∞ sLPV controllers design are the same as the designed ad-sLPV controller for fair comparison. Also, to show the effect of the smooth function of control transition, a controller denoted by d-sLPV is designed under the scheme formulated in this article without the smooth module, where the parameters are identical to the designed ad-sLPV controller.

Fig. 6 shows the state response and control input of the flight control system of *Firebee* under the different initial conditions, where subfigures (a)–(d) and subfigures (e)–(h) correspond to the initial condition $[\Delta\alpha, \Delta q]^T = [-0.1, 0.05]^T$, $[0.2, -0.05]^T$, respectively, which are slight perturbations in the rapid-switching T-portion to show the advantages of the proposed antibump sLPV controller.

Using common LPV and sLPV, peak values of 0.15 and 0.078 rad are obtained in Fig. 6(a), which implies a relatively great overshoot as compared to the steady state. By sLPV, the adjusting time for reaching the steady state is 3.569 s that is shorter than the one using LPV (6.066 s). Compared with both sLPV and LPV, the H_∞ sLPV, which treats the delayed scheduling on control inputs as disturbance, alleviates the great overshoot and reduces the adjusting time to the steady state since it obtains a small peak value of 0.003 rad and adjusting time of 2.389 s. Using the modeling approach proposed in this article, the d-sLPV controller and the ad-sLPV controller obtain better transient-state performance than the aforementioned controllers, where the peak values are 0.00226 and 0.00245 rad, while the adjusting time is 2.246 and 2.316 s, respectively. Using ad-sLPV, although the transient performance is a little lost (only as compared to d-sLPV), it obtains a more smoothly transitional control input than both d-sLPV controller and H_∞ sLPV controller, where the elevator deflection and the next-level actuator input are shown in Fig. 6(c) and (d), respectively. Fig. 6(e)–(h) are the state responses and control inputs under the initial value of $[0.2, -0.05]^T$, where the performance of ad-sLPV is the best as compared to other controllers in terms of smooth control inputs, small overshoot, and little adjusting time. Hence, for the transient performance, the effectiveness and advantages of the designed antibump sLPV controller for delayed scheduling (i.e., ad-sLPV) are demonstrated.

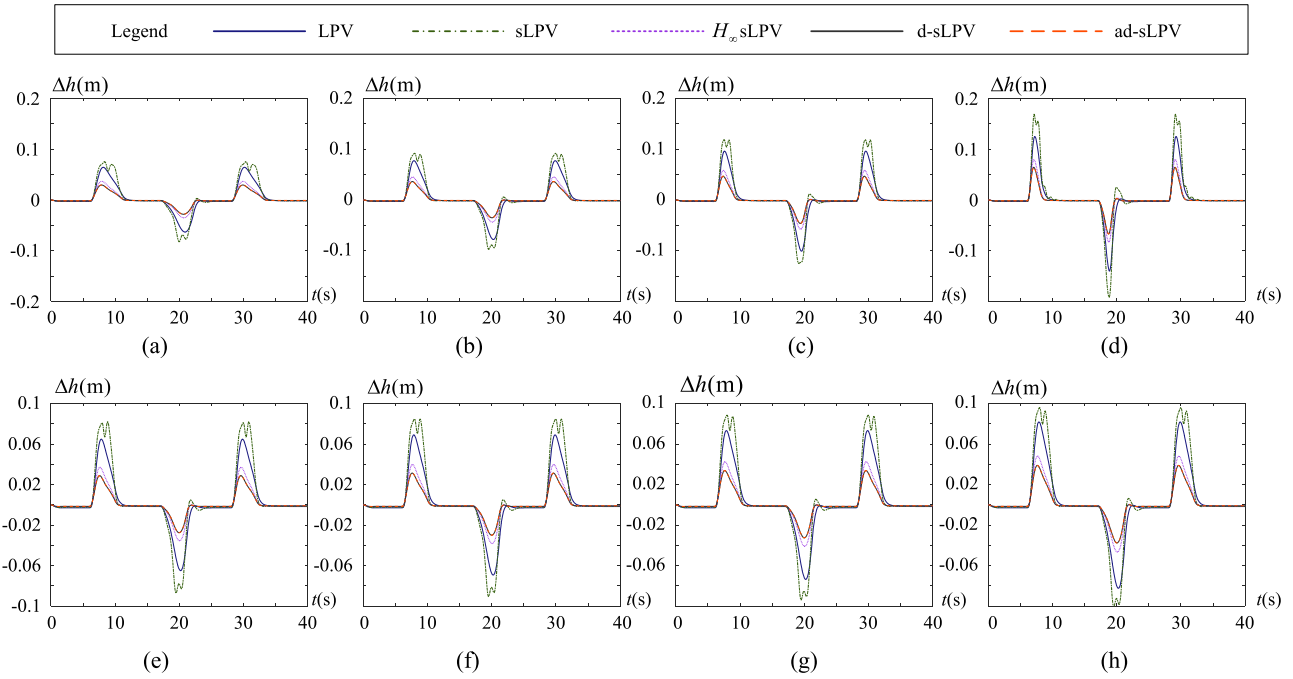


Fig. 7. Altitude variation of *Navion L-17* with delayed scheduling in the different cases of morphing speed and measurement delay, where the captions of subfigures (a, b) stand for the morphing duration $T_m = a$ and time lag of delayed scheduling $T_a = b$. The adopted controllers are obtained via the schemes include LPV, sLPV, and H_∞ sLPV in pervious studies, and d-sLPV (sLPV considering delayed scheduling) and ad-sLPV (antibump sLPV considering delayed scheduling) in this article. (a) (5, 0.05). (b) (4, 0.05). (c) (3, 0.05). (d) (2, 0.05). (e) (4, 0.02). (f) (4, 0.03). (g) (4, 0.04). (h) (4, 0.06).

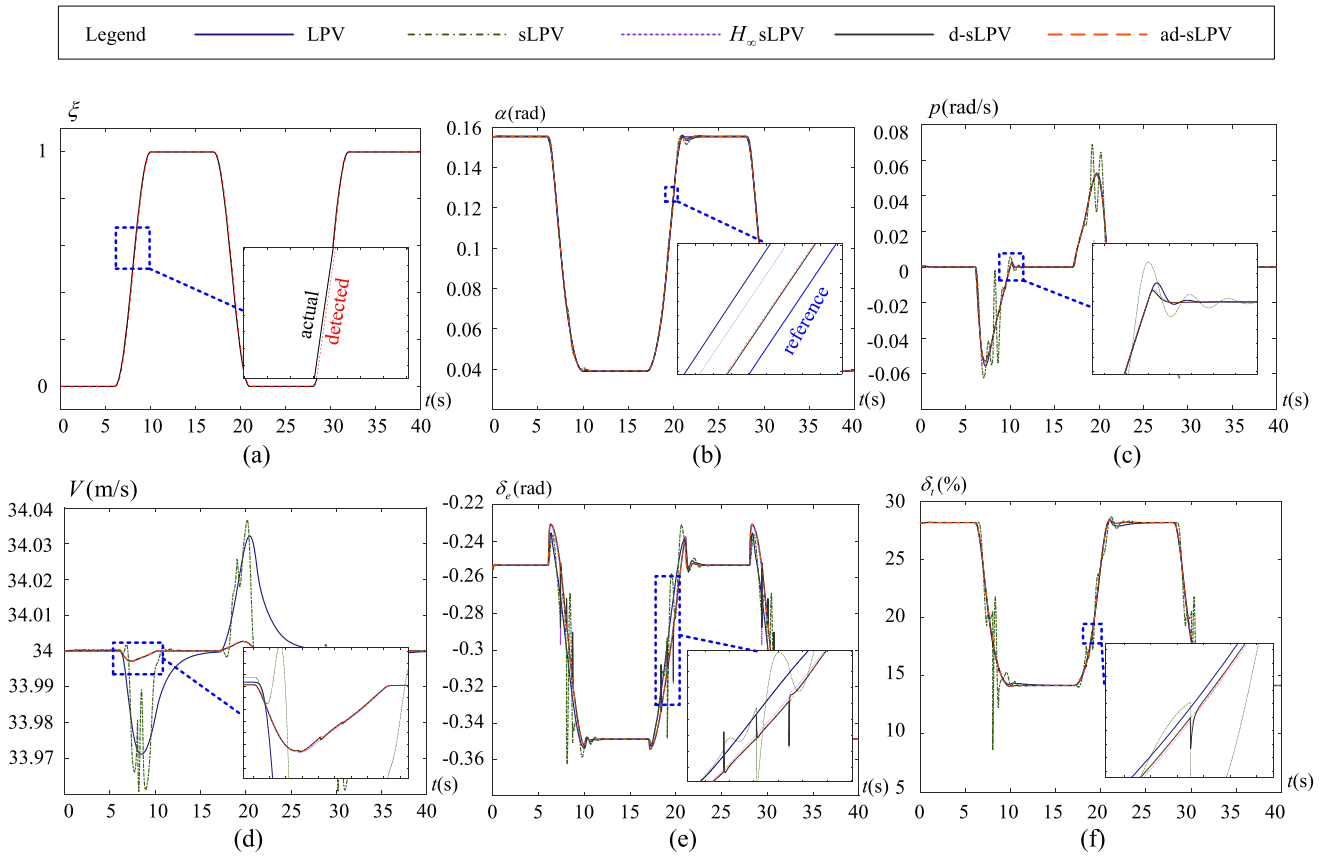


Fig. 8. Flight control performance of *Navion L-17* with delayed scheduling with the morphing duration $T_m = 4$ and time lag of delayed scheduling $T_a = 0.05$, where the adopted controllers are obtained via the schemes include LPV, sLPV, and H_∞ sLPV in pervious studies, and d-sLPV (sLPV considering delayed scheduling) and ad-sLPV (antibump sLPV considering delayed scheduling) in this article. (a) Morphing extent. (b) Attack angle. (c) Angle velocity. (d) Airspeed. (e) Elevator deflection. (f) Throttle valve opening.

B. Example 2: Dynamic Model of Navion L-17

In this example, the original dynamic model of morphing aircraft with a variable wingspan named *Navion L-17* [21] is utilized. The objectives here are to verify the control performance in a general scenario, where the aircraft in steady flight with the current structural configuration is required to rapidly deform to the another structural configuration and to keep steady flight again. The scheduling variable is defined as the morphing extent of the wingspan $\xi = \Delta b/b \in [0, 1]$, where Δb and b are the current and the maximum length of the wingspan, respectively, then the longitudinal dynamics of *Navion L-17* can be described by [22]

$$\begin{aligned}\dot{V} &= \frac{T_{\delta_t} \delta_t}{m} \cos \alpha - \frac{\rho V^2 S_w C_D(\xi, \alpha)}{2m} - g \sin(\theta - \alpha) \\ \dot{\alpha} &= q - \frac{T_{\delta_t} \delta_t}{mV} \sin \alpha - \frac{\rho V^2 S_w C_L(\xi, \alpha, \delta_e)}{2mV} + \frac{g}{V} \cos(\theta - \alpha) \\ \dot{\theta} &= q \\ \dot{q} &= \frac{\rho V^2 S_w c_A C_M(\xi, \alpha, \delta_e)}{2I_y} \\ \dot{h} &= V \sin(\theta - \alpha)\end{aligned}\quad (16)$$

where V , α , θ , q , and h are the states of the flight control system that refer to airspeed, attack angle, pitching angle, velocity of pitching angle, and altitude, respectively; δ_e and δ_t are the control inputs that stand for elevator deflection and throttle valve opening, respectively; $C_D(\xi, \alpha)$, $C_L(\xi, \alpha, \delta_e)$, and $C_M(\xi, \alpha, \delta_e)$ are the coefficients of corresponding axes related to the morphing extent of the wingspan; T_{δ_t} , m , S_w , g , ρ , c_A , and I_y are the constant parameters of *Navion L-17* that stand for thrust coefficient, mass, area of wing, gravity, air density, mean aerodynamic chord, moment of inertia of pitch, respectively (see [22] for more details). Considering that the aircraft is in steady flight at $h = 1524$ m and $V = 34$ m/s, then the LPV model can be formulated as

$$\begin{aligned}\begin{bmatrix} \Delta \dot{V} \\ \Delta \dot{\alpha} \\ \Delta \dot{\theta} \\ \Delta \dot{q} \\ \Delta \dot{h} \end{bmatrix} &= \begin{bmatrix} a_{11}(\xi) & a_{12}(\xi) & -9.8 & 0 & 0 \\ a_{21}(\xi) & a_{22}(\xi) & 0 & 1 & 0 \\ 0 & 0 & 0 & 1 & 0 \\ a_{41}(\xi) & a_{42}(\xi) & 0 & 0 & 0 \\ 0 & -34 & 34 & 0 & 0 \end{bmatrix} \begin{bmatrix} \Delta V \\ \Delta \alpha \\ \Delta \theta \\ \Delta q \\ \Delta h \end{bmatrix} \\ &+ \begin{bmatrix} 0 & 0.0331 \\ -0.0789 & 0 \\ 0 & 0 \\ -4.5436 & 0 \\ 0 & 0 \end{bmatrix} \begin{bmatrix} \Delta \delta_e \\ \Delta \delta_t \end{bmatrix}\end{aligned}\quad (17)$$

where the expression of $a_{ij}(\xi)$ ($i \in [1, 2, 4]$ and $j \in [1, 2]$) can be found in the Appendix, $\Delta q = q - 0$, $\Delta h = h - 0$, $\Delta \delta_e = \delta_e - 0.0196\xi^3 + 0.0604\xi^2 + 0.0548\xi + 0.2532$, and $\Delta \delta_t = \delta_t + 7.7211\xi^3 - 22.6867\xi^2 + 28.9719\xi - 28.1335$.

In the considered scenario, the aircraft keeps steady flight at minimum or maximum wingspan, and the structural configuration deforms rapidly between them. The range of the scheduling variable $\xi \in [0, 1]$ is split equally into

four partitions including $\xi \in [0, 0.25]$, $\xi \in [0.25, 0.5]$, $\xi \in [0.5, 0.75]$, and $\xi \in [0.75, 1]$, which indicates there are four modes denoted by 1, 2, 3, and 4, respectively. Considering the steady flight and rapid morphing requirements, the mode 1 and mode 4 only appear in the τ -portion, while the mode 2 and mode 3 shall be in the \mathbb{T} -portion.

The aircraft is required to achieve the rapid morphing via $\xi = 0.5 \sin(\frac{t-t_m}{T_m} \pi - \frac{\pi}{2}) + 0.5$, where t_m and T_m are the start time and total time of wingspan morphing, respectively. Suppose that the maximum morphing extent detection time delay is $\bar{T}_a \leq 0.06$ s and the maximum morphing speed is $\dot{\xi}_{\max} = 0.8$ /s, then the antibump sLPV controller for delayed scheduling (i.e., ad-sLPV) is designed via Theorem 1 with $\mu_{ij} = 1.2$, $[q_1, q_2, q_3, q_4] = [0.3, 0.1, 0.2, 0.3]$, $\gamma_0^2 = 0.1$ that has been optimized, $\varepsilon_{ij} = -q_i$, smooth function $\chi(t) = \sin[\frac{(t-t_m)}{T_s} \cdot \frac{\pi}{2}]$ with $T_s = 0.13$ s, where the asynchronous module covers 20% of the total partition to be reached. Then, the PDT condition $\tau > 5.1096$ and H_∞ performance $\gamma < 0.8248$ for the actual morphing process are obtained, which is suitable for any total morphing time T_m satisfying the physical constraints aforementioned. For the case that morphing time is quite great, the PDT switching signal will convert to the one with DT/ADT property, where the designed controller can also be used since the intractable rapid-switching \mathbb{T} -portion is avoided. On the contrary, it is difficult to use DT/ADT switching signals for controller design since the actual duration of modes 2 and 3 is quite small that requires relatively great q_i and small μ_i .

For comparison, three controllers in previous work, including common LPV [20], sLPV [7], and H_∞ sLPV [9], and a controller obtained via Theorem 1 without smooth module that is denoted by d-LPV in this article are utilized, where $\varrho = 0.1$ is used in the common LPV, and the parameters q_i , μ_{ij} , ε_{ij} , and γ_0 in corresponding schemes are the same as the designed ad-LPV controller for fair comparison.

The control performance is tested under different morphing conditions, including the rapid morphing duration $T_m = 2, 3, 4, 5$ s and the actual maximum time lag of the morphing extent detection $\bar{T}_a = 0.02, 0.03, 0.04, 0.05, 0.06$ s. The variations of altitude of *Navion L-17* under different morphing duration $T_m = 2, 3, 4, 5$ s and time lag $T_a = 0.05$ s are shown in Fig. 7(a)–(d), while Fig. 7(e)–(h) depict the altitude variations under same morphing duration $T_m = 4$ s and various time lag $T_a = 0.02, 0.03, 0.04, 0.06$ s. For the desired tracking error $\Delta h = 0$, the maximum tracking error is reduced when using ad-sLPV and d-sLPV, where they reduce the tracking error about 20%, 45%, and 60% as compared to H_∞ sLPV, sLPV, and LPV, respectively. It is obvious that using d-sLPV and ad-sLPV, lower tracking error of altitude can be obtained under any morphing speed and time lag as compared to other controllers. Specifically, from Fig. 7(a)–(d), the tracking error increases as the morphing duration decreases, while one can find that the tracking error decreases as the maximum time lag of morphing extent decrease from Fig. 7(e)–(h). The variations of the states and control inputs of *Navion L-17* under $T_m = 4$ s and $T_a = 0.05$ s are shown in Fig. 8,

where the morphing of the aircraft is shown in Fig. 8(a). Fig. 8(b) shows the state variation of attack angle, where the trim value is also related to the scheduling variable, and the designed ad-sLPV controller shows its superior capability on both tracking error alleviation in the morphing process and rapidly reaching the steady state when the morphing is completed. For the angle velocity in Fig. 8(c) and the airspeed in Fig. 8(d), a similar conclusion for steady-state performance, as demonstrated in the above subsection for transient-state performance, can be obtained that the controllers designed via H_∞ sLPV, d-sLPV, and ad-sLPV schemes achieve obviously better performance as compared to common LPV and sLPV. Also, the controllers designed via d-sLPV and ad-sLPV in this article achieve less tracking error than H_∞ sLPV in the presence of delayed scheduling, and ad-sLPV realizes a smooth transition as compared to the other controllers based on sLPV schemes, as shown in Fig. 8(e) and (f) for the elevator deflection angle and throttle valve opening, respectively.

Based on the LPV model of *Firebee* and the original dynamic model of *Navion L-17*, the effectiveness and the superiority of the formulated sLPV model for delayed scheduling via PDT switching signals and the corresponding antibump sLPV controller design method are verified.

VI. CONCLUSION

The issue of antibump sLPV controller design for morphing aircraft in the presence of delayed scheduling is investigated in this article. The delayed scheduling is formulated as the disturbance to control input and the asynchronous control for synchronous and asynchronous mode detection in sLPV, respectively, which has not been considered before. The mode switching is described via PDT switching signals, which are applicable to rapid morphing requirements and cover the conventional DT/ADT switching signals as special cases. The antibump sLPV controller design approach for the underlying system is carried out via a smooth function and detected-mode-based Lyapunov functions, where the effectiveness and the superiority are verified by simulations. The utilization of the proposed method on the practical morphing aircraft is worthwhile for further investigation. Also, the developed ideas and techniques can be extended to other unmanned systems with delayed measurements of scheduling variables of nonlinear dynamics related to plants themselves or the surrounding environments [23], [24], [25].

APPENDIX

A. Proof of Lemma 1

In the $(k-1)$ th mode of the p th stage, define the detected-mode-based Lyapunov functions in the \mathbb{T} -portion as $V_{p,k}$, and denote the start time of the m th divided intervals in the smooth module as $t_{p,k}^{s,m}$, where $m \in [0, n_s]$ and $t_{p,k}^{s,0} = t_{p,k}^a$, $t_{p,k}^{s,n_s} = t_{p,k}^s$. Then, $k \in [1, N_T]$ is included in the rapid-switching \mathbb{T} -portion, and $k=0$ appears in the τ -portion. In the \mathbb{T} -portion of the p th stage, for $\forall t \in [t_{p,n}^s, t_{p+1})$, $n < N_T$,

we can have that

$$\begin{aligned} V_{\sigma(t)}(t) &\leq V_{p,n}(t_{p,n}^s) e^{-\varrho_{p,n}(t-t_{p,n}^s)} \\ &\leq V_{p,n}(t_{p,n}^{s,n_s-1}) e^{\vartheta_{p,n}^{n_s-1}(t_{p,n}^s - t_{p,n}^{s,n_s-1})} e^{-\varrho_{p,n}(t-t_{p,n}^s)} \\ &\leq \dots \leq V_{p,n}(t_{p,n}^{s,0}) e^{\sum_{k=0}^{n_s-1} \vartheta_{p,n}^k T_s/n_s - \varrho_{p,n}(t-t_{p,n}^s)} \\ &\leq \mu_{p,n} V_{p,n-1}(t_{p,n}^a) e^{\sum_{k=0}^{N-1} \vartheta_{p,n}^k T_s/n_s - \varrho_{p,n}(t-t_{p,n}^s)} \\ &\leq \mu_{p,n} V_{p,n-1}(t_{p,n}) e^{\varepsilon_{p,n}(t_{p,n}^a - t_{p,n})} \\ &\quad \times e^{\sum_{k=0}^{N-1} \vartheta_{p,n}^k T_s/n_s - \varrho_{p,n}(t-t_{p,n}^s)} \leq \dots \\ &\leq V_{p,1}(t_{p,1}) \prod_{k=1}^{N_T} \mu_{p,k} e^{\varepsilon_{p,k}(t_{p,k}^a - t_{p,k}) + \sum_{m=0}^{n_s-1} \vartheta_{p,k}^m T_s/n_s} \\ &\leq \bar{\mu}^{N_T} V_{p,0}(t_{p,1}) e^{N_T \cdot (\bar{\varepsilon} \bar{T}_a + \sum_{m=0}^{n_s-1} \bar{\vartheta}^m T_s/n_s)} \\ &\leq V_{p,0}(t_{p,1}) e^{N_T (ln \bar{\mu} + \bar{\varepsilon} \bar{T}_a + T_s \Xi(\bar{\vartheta}^m, n_s))}. \end{aligned}$$

Then, in the τ -portion of p -stage with DT τ_p , we have

$$\begin{aligned} V_{p,0}(t_{p,1}) &\leq \mu_{p,0} V_{p-1,n}(t_{p,0}) e^{\varepsilon_{p,0} \bar{T}_a + T_s \Xi(\vartheta_{p,0}^m, n_s) - \varrho_{p,0}(t_{p,1} - t_{p,0}^s)} \\ &\leq \mu_{p,0} V_{p-1,n}(t_{p,0}) e^{(\varepsilon_{p,0} + \varrho_{p,0}) \bar{T}_a + T_s \Xi(\varrho_{p,0}, \vartheta_{p,0}^m, n_s) - \varrho_{p,0} \tau_p}. \end{aligned}$$

Thus, in the p th stage, one has

$$\begin{aligned} V_{\sigma(t)}(t) &\leq \bar{\mu}^{N_T} \mu_{p,0} V_{p-1,n}(t_{p,0}) e^{(\varepsilon_{p,0} + \varrho_{p,0}) \bar{T}_a + T_s \Xi(\varrho_{p,0}, \vartheta_{p,0}^m, n_s)} \\ &\quad \times e^{N_T (ln \bar{\mu} + \bar{\varepsilon} \bar{T}_a + T_s \Xi(\bar{\vartheta}^m, n_s))} \times e^{-\varrho_{p,0} \tau_p}. \end{aligned}$$

Let $\lambda_p = N_T ln \bar{\mu} + ln \mu_{p,0} + (\varepsilon_{p,0} + \varrho_{p,0}) \bar{T}_a - \varrho_{p,0} \tau_p + N_T \bar{\varepsilon} \bar{T}_a + T_s \Xi(N_T \bar{\vartheta}^m, \varrho_{p,0}, \vartheta_{p,0}^m, n_s) \leq f(ln \bar{\mu} + (\bar{\varepsilon} + \varrho) + T_s \Xi(\varrho, \bar{\vartheta}^m, n_s)) - \varrho \tau$, then we have the PDT condition (7), and the system energy variation as the stage evolution follows that

$$V_{\sigma(t)}(t) \leq e^{\lambda_p} V_{\sigma(t_p)}(t_p) \leq \dots \leq e^{\lambda_p + \lambda_{p-1} + \dots + \lambda_0} V_{\sigma(0)}(t_0)$$

which ensures the stability of the underlying system. ■

B. Proof of Lemma 2

By using the same definitions of time instants as Appendix A, for the p th stage, consider $w(t) \neq 0$, we have

$$\begin{aligned} V_{\sigma(t)}(t) &\leq V_{p,n}(t_{p,n}^s) e^{-\varrho_{p,n}(t-t_{p,n}^s)} - \int_{t_{p,n}^s}^t e^{-\varrho_{p,n}(t-l)} \Gamma(l) dl \\ &\leq \left[V_{p,n}(t_{p,n}^{s,n_s-1}) e^{\vartheta_{p,n}^{n_s-1} T_s/n_s} - \int_{t_{p,n}^{s,n_s-1}}^{t_{p,n}^s} e^{\vartheta_{p,n}^{n_s-1}(t_{p,n}^s - l)} \right. \\ &\quad \left. \times \Gamma(l) dl \right] e^{-\varrho_{p,n}(t-t_{p,n}^s)} - \int_{t_{p,n}^s}^t e^{-\varrho_{p,n}(t-l)} \Gamma(l) dl \\ &\leq V_{p,n}(t_{p,n}^{s,n_s-1}) e^{\vartheta_{p,n}^{n_s-1} T_s/n_s - \varrho_{p,n}(t-t_{p,n}^s)} - e^{-\varrho_{p,n}(t-t_{p,n}^s)} \\ &\quad \times \int_{t_{p,n}^{s,n_s-1}}^{t_{p,n}^s} e^{\vartheta_{p,n}^{n_s-1}(t_{p,n}^s - l)} \Gamma(l) dl - \int_{t_{p,n}^s}^t e^{-\varrho_{p,n}(t-l)} \Gamma(l) dl \\ &\leq \dots \leq V_{p,n}(t_{p,n}^{s,0}) e^{\sum_{k=0}^{n_s-1} \vartheta_{p,n}^k T_s/n_s - \varrho_{p,n}(t-t_{p,n}^s)} \\ &\quad - e^{\sum_{k=1}^{n_s-1} \vartheta_{p,n}^k T_s/n_s - \varrho_{p,n}(t-t_{p,n}^s)} \int_{t_{p,n}^{s,0}}^{t_{p,n}^s} e^{\vartheta_{p,n}^1(t_{p,n}^{s,1} - l)} \Gamma(l) dl \end{aligned}$$

$$\begin{aligned}
& \times \Gamma(l)dl - \dots - e^{-\underline{\varrho}_{p,n}(t-t_{p,n}^s)} \int_{t_{p,n}^{s-1}}^{t_{p,n}^s} e^{\vartheta_{p,n}^{s-1}(t_{p,n}^s-l)} \Gamma(l)dl \\
& - \int_{t_{p,n}^s}^t e^{-\underline{\varrho}_{p,n}(t-l)} \Gamma(l)dl \\
& \leq \mu_{p,n} V_{p,n-1}(t_{p,n}^a) e^{\sum_{k=0}^{n_s-1} \vartheta_{p,n}^k \frac{T_s}{n_s} - \underline{\varrho}_{p,n}(t-t_{p,n}^s)} - \dots \\
& - \int_{t_{p,n}^s}^t e^{-\underline{\varrho}_{p,n}(t-l)} \Gamma(l)dl \\
& \leq \mu_{p,n} V_{p,n-1}(t_{p,n}) e^{\varepsilon_{p,n}(t_{p,n}^a - t_{p,n}) + \sum_{k=0}^{n_s-1} \vartheta_{p,n}^k \frac{T_s}{n_s} - \underline{\varrho}_{p,n}(t-t_{p,n}^s)} \\
& - \mu_{p,n} e^{\sum_{k=0}^{n_s-1} \vartheta_{p,n}^k \frac{T_s}{n_s} - \underline{\varrho}_{p,n}(t-t_{p,n}^s)} \int_{t_{p,n}}^{t_{p,n}^a} e^{\varepsilon_{p,n}(t_{p,n}^a-l)} \Gamma(l)dl \\
& - e^{\sum_{k=0}^{n_s-1} \vartheta_{p,n}^k \frac{T_s}{n_s} - \underline{\varrho}_{p,n}(t-t_{p,n}^s)} \int_{t_{p,n}^a}^{t_{p,n}^{s,1}} e^{\vartheta_{p,n}^1(t_{p,n}^{s,1}-l)} \Gamma(l)dl \\
& - \dots - \int_{t_{p,n}^s}^t e^{-\underline{\varrho}_{p,n}(t-l)} \Gamma(l)dl.
\end{aligned}$$

By considering the zero initial condition and the worst case as Lemma 1, one can conclude

$$\int_{t_0}^t \bar{\mu}^N(t,l) e^{-\underline{\varrho} T_{\text{syn}}(t,l) + \bar{\varepsilon} T_{\text{asy}}(t,l) + \Xi(\bar{\vartheta}^m, n_s) T_{\text{smo}}(t,l)} \Gamma(l)dl \leq 0$$

where $N(l, t)$ is the switching times between l and t , while $T_{\text{syn}}(l, t)$, $T_{\text{asy}}(l, t)$, and $T_{\text{smo}}(l, t)$ are the total time of the synchronous module, asynchronous module, and smooth module, respectively, between l and t . By denoting a factor $\iota = \frac{f}{\bar{\tau}} \leq \frac{f}{\tau + T_{\text{as}}}$, then, we have

$$\begin{aligned}
0 & \leq N(t, l) \leq (t-l)\iota + f \\
0 & \leq T_{\text{asy}}(l, t) \leq (t-l)\iota \bar{T}_a + f \bar{T}_a \\
0 & \leq T_{\text{smo}}(l, t) \leq (t-l)\iota T_s + f T_s.
\end{aligned}$$

For $\Gamma(l) = \|z(l)\|^2 - \gamma_0^2 \|w(l)\|^2$, one has

$$\begin{aligned}
\int_{t_0}^t e^{-\underline{\varrho}(t-l)} \|z(l)\|^2 dl & \leq \gamma_0^2 \int_{t_0}^t \bar{\mu}^{(t-l)\iota + f} \times e^{-\underline{\varrho}(t-l)} \\
& \times e^{(\underline{\varrho} + \bar{\varepsilon})[(t-l)\iota + f] \bar{T}_a + (t-l)\iota + f] \Xi(\underline{\varrho}, \bar{\vartheta}^m, n_s) T_s} \|w(l)\|^2 dl
\end{aligned}$$

Let $c_0 = \bar{\mu}^f e^{(\underline{\varrho} + \bar{\varepsilon})f \bar{T}_a + f \Xi(\underline{\varrho}, \bar{\vartheta}^m, n_s) T_s}$ and $c_1 = \ln \bar{\mu} - \underline{\varrho} + (\underline{\varrho} + \bar{\varepsilon})\iota \bar{T}_a + \iota \Xi(\underline{\varrho}, \bar{\vartheta}^m, n_s) T_s$, then, we have

$$\int_{t_0}^t e^{-\underline{\varrho}(t-l)} \|z(l)\|^2 dl \leq c_0 \gamma_0^2 \int_{t_0}^t e^{c_1(t-l)} \|w(l)\|^2 dl.$$

It follows that

$$\int_0^\infty \int_{t_0}^t e^{-\underline{\varrho}(t-l)} \|z(l)\|^2 dl dt \leq c_0 \gamma_0^2 \int_0^\infty \int_{t_0}^t e^{c_1(t-l)} \|w(l)\|^2 dl dt$$

which equals to

$$\int_{t_0}^\infty \int_l^\infty e^{-\underline{\varrho}(t-l)} \|z(l)\|^2 dl dt \leq c_0 \gamma_0^2 \int_{t_0}^\infty \int_l^\infty e^{c_1(t-l)} \|w(l)\|^2 dl dt$$

one has

$$\int_{t_0}^\infty \frac{1}{\underline{\varrho}} \|z(t)\|^2 dt \leq c_0 \gamma_0^2 \int_{t_0}^\infty -\frac{1}{c_1} \|w(t)\|^2 dt.$$

Thus, we have

$$\int_{t_0}^\infty \|z(t)\|^2 dt \leq -\frac{c_0 \underline{\varrho}}{c_1} \gamma_0^2 \int_{t_0}^\infty \|w(t)\|^2 dt.$$

Hence, the parameter c in \mathcal{L}_2 gain from $\gamma = c\gamma_0 = \sqrt{-\frac{c_0 \underline{\varrho}}{c_1}} \gamma_0$ can be concluded as (9), which ends the proof. ■

C. Proof of Theorem 1

Consider the detected-mode-based Lyapunov functions $V_i = x^T P_i x$, for the synchronous module, to satisfy (10), the following inequality shall be ensured:

$$\begin{aligned}
\dot{V}_i(t) + \varrho_i V_i(t) + z^T(t)z(t) - \gamma_0^2 w^T(t)w(t) & = x^T(t)P_i \bar{A}_i(\xi) \\
& \times x(t) + B^w w(t) + (\bar{A}_i(\xi)x(t) + B^w w(t))^T P_i x(t) \\
& + \varrho_i x^T(t)P_i x(t) + (Cx(t))^T (Cx(t)) - \gamma_0^2 w^T(t)w(t) \\
& = \begin{bmatrix} x(t) \\ w(t) \end{bmatrix}^T \begin{bmatrix} P_i \bar{A}_i(\xi) + \bar{A}_i^T(\xi)P_i + \varrho_i P_i + C^T C & P_i B^w \\ \star & -\gamma_0^2 I \end{bmatrix} \\
& \times \begin{bmatrix} x(t) \\ w(t) \end{bmatrix} < 0
\end{aligned} \tag{18}$$

which equals to

$$\begin{bmatrix} P_i \bar{A}_i(\xi) + \bar{A}_i^T(\xi)P_i + \varrho_i P_i + C^T C & P_i B^w \\ \star & -\gamma_0^2 I \end{bmatrix} < 0$$

then, we have

$$\begin{aligned}
& \begin{bmatrix} P_i \bar{A}_i(\xi) + \bar{A}_i^T(\xi)P_i + \varrho_i P_i & P_i B^w \\ \star & -\gamma_0^2 I \end{bmatrix} \\
& - \begin{bmatrix} C_i^T(\xi) \\ 0 \end{bmatrix} (-I) [C_i(\xi) \quad 0] < 0.
\end{aligned}$$

Using the lemma of Schur complements, one has

$$\begin{bmatrix} P_i \bar{A}_i(\xi) + \bar{A}_i^T(\xi)P_i + \varrho_i P_i & P_i B^w & C^T \\ \star & -\gamma_0^2 I & 0 \\ \star & \star & -I \end{bmatrix} < 0.$$

By contragradient transformation via $\text{diag}\{P_i^{-1}, I, I\}$, one has the following inequality shall be negative-definite:

$$\begin{bmatrix} \bar{A}_i(\xi)P_i^{-1} + P_i^{-1}\bar{A}_i^T(\xi) + \varrho_i P_i^{-1} & B^w & P_i^{-1}C^T \\ \star & -\gamma_0^2 I & 0 \\ \star & \star & -I \end{bmatrix}.$$

By considering $\bar{A}_i(\xi) = A_i(\xi) + BK_i(\xi)$, and letting $X_i = P_i^{-1}$, $W_i(\xi) = K_i(\xi)P_i^{-1}$, one has

$$\mathcal{H}(A_i(\xi)X_i + BW_i(\xi) + X_i A_i^T(\xi) + W_i^T(\xi)B + \varrho_i X_i, X_i) < 0. \tag{19}$$

Considering the property of polytopic system $A_i(\xi) = \sum \varpi_i A^k$ and $W_i(\xi) = \sum \varpi_i W^k$, the first inequality of (10) can be obtained.

As for the asynchronous module, following the similar operation as (18) to (19), and considering $\bar{A}_{ij}^a(\xi) = A_{ij}^a(\xi) + BK_j(\xi^d)$, $\dot{V}_i(t) - \varepsilon_{ij} V_i(t) + z^T(t)z(t) - \gamma_0^2 w^T(t)w(t) < 0$

equals to $\mathcal{H}(A_{ij}^a(\xi)X_i + BW_i(\xi^d) + X_iA_{ij}^{aT}(\xi) + W_i^T(\xi^d)B - \varepsilon_{ij}X_i, X_i) < 0$. For $\forall \xi$ in mode j , the above inequality can be ensured via the vertex combination of ξ^d in mode i if the following condition holds:

$$\mathcal{H}(A_{ij}^a(\xi)X_i + BW_i^r + X_iA_{ij}^{aT}(\xi) + W_i^{rT}B - \varepsilon_{ij}X_i, X_i) < 0$$

where $W_i(\xi^d) = \sum \varpi_i(\xi^d)W_i^r$. By further considering the polytopic system for the asynchronous module, i.e., $A_{ij}^a(\xi) = \sum \varpi_{ij}^a A_j^k$, where ϖ_{ij}^a corresponds to the weights ϖ_j that varies in the asynchronous module of the mode j , then, the second inequality in (10) can be obtained.

For the smooth module, we use a smooth function $\chi(t)$ such that control gains transition from the final gains: $K_i(\xi_{ij}^b) = \sum \varpi_i(\xi_{ij}^b)K_i^k = \sum \varpi_i(\xi_{ij}^b)W_i^k X_i^{-1}$ in mode i to the detected-scheduling-variables-dependent gains: $K_j(\xi^d) = \sum \varpi_j(\xi^d)K_j^k = \sum \varpi_j(\xi^d)W_j^k X_j^{-1}$ in mode j . From (11), for the scalar μ_{ij}^s , we have

$$\mathcal{H}(\bar{A}_{ij}^s(\xi)X_j + X_j\bar{A}_{ij}^{sT}(\xi) - \mu_{ij}^s X_j, X_j) < 0$$

where $\bar{A}_{ij}^s(\xi) = A_{ij}^s(\xi) + BK_i(\xi_{ij}^b)$ that reflects the effect of $K_i(\xi_{ij}^b)$ on the $A_j(\xi)$ in the smooth module of the mode j . Considering $\mathcal{H}(\bar{A}_j(\xi)X_j + X_j\bar{A}_j^T(\xi) + \varrho_j X_j, X_j) < 0$ adapted from (19) for mode j and $A_{ij}^s(\xi) \subseteq A_j(\xi)$, we have

$$(1 - \chi(t))\mathcal{H}(\bar{A}_{ij}^s(\xi)X_j + X_j\bar{A}_{ij}^{sT}(\xi) - \mu_{ij}^s X_j, X_j) + \chi(t)\mathcal{H}(\bar{A}_j(\xi)X_j + X_j\bar{A}_j^T(\xi) + \varrho_j X_j, X_j) < 0$$

which equals to

$$\mathcal{H}((A_{ij}^s(\xi) + B(\chi(s(t))K_j(\xi) + (1 - \chi(t))K_i(\xi_{ij}^b)))X_j + X_j(A_{ij}^s(\xi) + B(\chi(s(t))K_j(\xi) + (1 - \chi(t))K_i(\xi_{ij}^b)))^T + \chi(t)\varrho_j - (1 - \chi(s(t)))\mu_{ij}^s X_j, X_j) < 0.$$

For the monotonically increasing function $\chi(t)$, we have $\chi(m\frac{T_s}{n_s}) \leq \chi(t)$ for $\forall t$ in the $(m+1)$ th interval of $t \in [m\frac{T_s}{n_s}, (m+1)\frac{T_s}{n_s}]$. Then, in the $(m+1)$ th interval, by letting $\vartheta_{ij}^m = \chi(m\frac{T_s}{n_s})\varrho_j - (1 - \chi(m\frac{T_s}{n_s}))\mu_{ij}^s$, one can have that (11) can be ensured by the designed controller (13) in the smooth module with the disturbance $\chi(t)(K_j(\xi^d) - K_j(\xi))x(t)$, i.e., $\dot{V}_i - \vartheta_{ij}^m V_i + z^T(t)z(t) - \gamma_0^2 w^T(t)w(t) < 0$.

Then, consider the inequality $X_i < \mu_{ij} X_j$, we have $P_j < \mu_{ij} P_i$, i.e., $V_j(x(t_j^a)) < \mu_{ij} V_i(x(t_j^a))$ at the detected switching instants. Hence, all the necessary conditions in Lemma 2 are achieved, so the sLPV controller obtained in this theorem satisfies the PDT conditions (7) and H_∞ performance (9), then the proof is completed. ■

D. Parameters of LPV Models in Simulation

Parameters in LPV model of *Firebee*

$$\begin{aligned} a_{11}(\xi) &= 0.2255\xi - 1.3967 \\ a_{21}(\xi) &= 0.0876\xi^2 - 0.4889\xi - 0.3775 \\ a_{22}(\xi) &= 0.4489\xi - 0.8229 \\ b_{11}(\xi) &= 0.00034\xi - 0.001638 \\ b_{21}(\xi) &= 0.000053\xi^2 - 0.044151\xi - 0.143984. \end{aligned}$$

Parameters in LPV model of *Navion L-17*

$$\begin{aligned} a_{11}(\xi) &= -0.0081\xi - 0.0056 \\ a_{12}(\xi) &= -0.7190\xi + 4.4794 \\ a_{21}(\xi) &= -0.0036\xi - 0.0109 \\ a_{22}(\xi) &= -1.4225\xi - 1.4559 \\ a_{41}(\xi) &= -0.0661\xi + 0.0049 \\ a_{42}(\xi) &= -5.9986\xi - 7.9386. \end{aligned}$$

ACKNOWLEDGMENT

The authors would like to acknowledge Dr. Roeland De Breuker for hosting and supporting the first author at Delft University of Technology.

REFERENCES

- [1] T. A. Weisshaar, "Morphing aircraft systems: Historical perspectives and future challenges," *J. Aircr.*, vol. 50, no. 2, pp. 337–353, 2013.
- [2] P. Dai, B. Yan, T. Han, and S. Liu, "Barrier Lyapunov function based model predictive control of a morphing waverider with input saturation and full state constraints," *IEEE Trans. Aerosp. Electron. Syst.*, vol. 59, no. 3, pp. 3071–3081, Jun. 2023.
- [3] T. Oktay and C. Sultan, "Comfortable helicopter flight via passive/active morphing," *IEEE Trans. Aerosp. Electron. Syst.*, vol. 51, no. 4, pp. 2876–2886, Oct. 2015.
- [4] V. L. Stuber, T. Mkhoyan, R. De Breuker, and S. van der Zwaag, "In-situ boundary layer transition detection on multi-segmental (a) synchronous morphing wings," *Meas. Sensors*, vol. 19, 2022, Art. no. 100356.
- [5] B. Sun, T. Mkhoyan, E.-J. van Kampen, R. De Breuker, and X. Wang, "Vision-based nonlinear incremental control for a morphing wing with mechanical imperfections," *IEEE Trans. Aerosp. Electron. Syst.*, vol. 58, no. 6, pp. 5506–5518, Dec. 2022.
- [6] B. Lu, F. Wu, and S. Kim, "Switching LPV control of an F-16 aircraft via controller state reset," *IEEE Trans. Control Syst. Technol.*, vol. 14, no. 2, pp. 267–277, Mar. 2006.
- [7] Y. Hou, Q. Wang, and C. Dong, "Gain scheduled control: Switched polytopic system approach," *J. Guid. Control Dyn.*, vol. 34, no. 2, pp. 623–629, 2011.
- [8] W. Jiang, C. Dong, and Q. Wang, "A systematic method of smooth switching LPV controllers design for a morphing aircraft," *Chin. J. Aeronaut.*, vol. 28, no. 6, pp. 1640–1649, 2015.
- [9] L. Zhang, L. Nie, B. Cai, S. Yuan, and D. Wang, "Switched linear parameter-varying modeling and tracking control for flexible hypersonic vehicle," *Aerosp. Sci. Technol.*, vol. 95, 2019, Art. no. 105445.
- [10] D. Yang, G. Zong, and H. R. Karimi, " H_∞ refined antidisturbance control of switched LPV systems with application to aero-engine," *IEEE Trans. Ind. Electron.*, vol. 67, no. 4, pp. 3180–3190, Apr. 2020.
- [11] J. P. Hespanha, "Uniform stability of switched linear systems: Extensions of LaSalle's invariance principle," *IEEE Trans. Autom. Control*, vol. 49, no. 4, pp. 470–482, Apr. 2004.
- [12] H. Shen, M. Xing, Z.-G. Wu, S. Xu, and J. Cao, "Multiobjective fault-tolerant control for fuzzy switched systems with persistent dwell time and its application in electric circuits," *IEEE Trans. Fuzzy Syst.*, vol. 28, no. 10, pp. 2335–2347, Oct. 2020.
- [13] P.-C. Chen, "The design of smooth switching control with application to VSTOL aircraft dynamics under input and output constraints," *Asian J. Control*, vol. 14, no. 2, pp. 439–453, 2012.
- [14] S. Shi, Z. Shi, and Z. Fei, "Asynchronous control for switched systems by using persistent dwell time modeling," *Syst. Control. Lett.*, vol. 133, Art. no. 104523, 2019.
- [15] S. Yuan, L. Zhang, and S. Baldi, "Adaptive stabilization of impulsive switched linear time-delay systems: A piecewise dynamic gain approach," *Automatica*, vol. 103, pp. 322–329, 2019.

- [16] Y. Liang, J. Yang, L. Zhang, S. Baldi, and B. De Schutter, "Switched control design for quadrotor in target tracking with complex intermittent measurements," *J. Guid. Control Dyn.*, vol. 46, no. 1, pp. 206–214, 2023.
- [17] J. P. Hespanha, "Root-mean-square gains of switched linear systems," *IEEE Trans. Autom. Control*, vol. 48, no. 11, pp. 2040–2045, Nov. 2003.
- [18] T. M. Seigler, "Dynamics and control of morphing aircraft," Ph.D. dissertation, Virginia Polytech. Inst. State Univ., Virginia Tech, Blacksburg, VA, USA, 2005.
- [19] W. Xu, Y. Li, M. Lv, and B. Pei, "Modeling and switching adaptive control for nonlinear morphing aircraft considering actuator dynamics," *Aerosp. Sci. Technol.*, vol. 122, 2022, Art. no. 107349.
- [20] J.-W. Van Wingerden, P. Gebraad, and M. Verhaegen, "LPV identification of an aeroelastic flutter model," in *Proc. IEEE Conf. Decis. Control*, 2010, pp. 6839–6844.
- [21] R. C. Nelson et al. *Flight Stability and Automatic Control*. New York, USA: WCB/McGraw Hill, 1998, vol. 2.
- [22] M. Yin, Y. Lu, and Z. He, "LPV modeling and robust gain scheduling control of morphing aircraft," *J. Nanjing Univ. Aeronaut. Astronaut.*, vol. 45, no. 2, pp. 202–208, 2013.
- [23] R. Cao, Y. Liu, and Y. Lu, "Robust multiple model predictive control for ascent trajectory tracking of aerospace vehicles," *IEEE Trans. Aerosp. Electron. Syst.*, vol. 58, no. 2, pp. 1333–1351, Apr. 2022.
- [24] D. Yang and J. Zhao, " H_∞ output tracking control for a class of switched LPV systems and its application to an aero-engine model," *Int. J. Robust Nonlinear Control*, vol. 27, no. 12, pp. 2102–2120, 2017.
- [25] W. Fan, H. H. Liu, and R. H. Kwong, "Gain-scheduling control of flexible aircraft with actuator saturation and stuck faults," *J. Guid. Control Dyn.*, vol. 40, no. 3, pp. 510–520, 2017.



Ye Liang (Member, IEEE) received the B.S. degree in automation from Northeast Forestry University (NEFU), Harbin, China, in 2017, the M.S. degree in control science and engineering and the Ph.D. degree in aeronautical and astronautical science and technology from the Harbin Institute of Technology, Harbin, China, in 2019 and 2023, respectively.

During his Ph.D., he was a visiting Ph.D. student with the Faculty of Aerospace Engineering, Delft University of Technology, Delft, Netherlands, from 2022 to 2023. He is currently an Associate Professor with the College of Computer and Control Engineering, NEFU. His research interests include switched systems and their applications to aircraft.

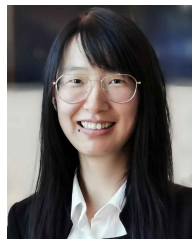


Lixian Zhang (Fellow, IEEE) received the Ph.D. degree in control science and engineering from the Harbin Institute of Technology, Harbin, China, in 2006.

From 2007 to 2008, he was a Postdoctoral Fellow with the Department Mechanical Engineering, Ecole Polytechnique de Montreal, Montreal, QC, Canada. He was a Visiting Professor with the Process Systems Engineering Laboratory, Massachusetts Institute of Technology, Cambridge, MA, USA, from 2012 to 2013. Since

2009, he has been with the Harbin Institute of Technology, where he is currently a Full Professor with the School of Astronautics. His research interests include multimodal systems, model predictive control, and their applications in the field of specialized robots.

Dr. Zhang was the recipient of the National Science Foundation for Distinguished Young Scholars of China. He serves as Senior Editor for IEEE CONTROL SYSTEMS LETTERS, and served as Associate Editor for IEEE TRANSACTIONS ON AUTOMATIC CONTROL and IEEE TRANSACTIONS ON CYBERNETICS. He was named to the list of Clarivate Highly Cited Researchers in 2016–2021.



Xuerui Wang received the Ph.D. degree in aerospace engineering from the Delft University of Technology (TUD), Delft, the Netherlands, in 2019.

From 2019 to 2020, she undertook a postdoctoral research position with Smart and Aeroelastic Structure Laboratory, TUD, where she was an Assistant Professor with the Faculty of Aerospace Engineering, in 2020. Her tenure track was jointly sponsored by the departments of control and operations and aerospace structures

and materials, leading to her tenure in 2023. Her research interests include nonlinear control, aeroelasticity, aerial robotics, and active morphing structures.

Dr. Wang is a member of the AIAA-Guidance, Navigation, and Control and International Federation of Automatic Control-Automatic Control in Aerospace technical committees and chairs technical sessions at AIAA SciTech in 2024 and 2025.